Structural, ultrastructural and immunohistochemical analysis of the vesicular gland in the male greater cane rat (*Thryonomys swinderianus*)

Adenrele O. Adebayo[1,2,3]**, Adebayo K. Akinloye**[2]**, Samuel G. Olukole**[1]**, Amadi O. Ihunwo**[3] **and Bankole O. Oke**[1]

[1]*Department of Veterinary Anatomy, Faculty of Veterinary Medicine, University of Ibadan, Ibadan, Nigeria,*
[2]*Department of Veterinary Anatomy, College of Veterinary Medicine, Federal University of Agriculture, Abeokuta, P.M.B 2240, Abeokuta, Nigeria and* [3]*School of Anatomical Sciences, Faculty of Health Sciences, University of the Witwatersrand, Johannesburg, South Africa*

SUMMARY

This study reports the structure, ultrastructure, morphometry and distribution patterns of the two estrogen receptors in the vesicular glands of the male greater cane rat. Samples of vesicular glands from 15 sexually mature male greater cane rats raised in captivity were routinely processed for histological, ultrastructural and morphometric analysis, while immunohistochemistry was also carried out using rabbit polyclonal antibodies against estrogen receptors.

The vesicular gland in the greater cane rat is a paired transparent elongated branched tube that presents a characteristic Y-shaped outline. The tube is made up of three histological layers: mucosa, muscularis and adventitia with the mucosa thrown into branching and anastomosing folds that form cavities and recesses within it. Though the epithelium is lined by principal and scarce basal cells, the principal cells are, however, of two types - light and dense based on their electron density and cytoplasmic characteristics. A prominent ultrastructural feature of the light principal cells is the presence of abundant mitochondria surrounded by well-developed cisternae of rough endoplasmic reticulum that have dilated edges and small vesicular extensions. The epithelial cells exhibited different patterns of expressions of estrogen receptor alpha (ERα) and estrogen receptor beta (ERβ). The findings highlight the peculiarities in the structure, ultrastructure and distribution of the estrogen receptors of the vesicular gland of greater cane rat.

Key words: Vesicular gland – Greater cane rat – Ultrastructure – Estrogen receptors

INTRODUCTION

The vesicular gland is one of the male accessory sex glands that produce and elaborate abundant amount of fluids for the transportation and nourishment of spermatozoa in the seminal plasma, as well as the formation of a vaginal stopper in some rodents (Chaves, et al., 2011). In pigs, these glands produce 80-90% of the seminal plasma proteins that protect and increase sperm viability and fertilizing capacity (Badia et al., 2006). Therefore, information on the morpho-physiology of these glands is imperative especially in wild species that are undergoing domestication and captive -rearing (Adaro et al., 2001; Chaves et al., 2012).

The varying functions of the vesicular gland are reflected in its structural and ultra-structural varia-

Corresponding author: Adenrele O. Adebayo. Department of Veterinary Anatomy, Federal University of Agriculture, P.M.B 2240, Abeokuta Nigeria. Tel: +234-805-090-0685; +234-803-594-0092. E-mail: releadebayo@yahoo.com; adebayoao@unaab.edu.ng

tions in the different mammalian species. While this gland is absent in some species (Strzezek et al., 2000), it shows structural variations across species where it is present. In humans, horses and rats they are saccularly shaped; in pigs and bulls they are compact and multilobulated (Samuelson, 2007; Badia et al., 2006), and in some rodent species they exhibit a branched tubular structure (Mollineau et al., 2009; Ayres de Menezes et al., 2010). There are also species variations in the presence and pattern of distribution of factors that mediate and regulate functions in these glands (Joseph et al., 2011).

It has been established that the normal development, differentiation and functioning of the vesicular gland (as well as the entire segments of the male reproductive tract) are regulated by the active form of testosterone, dihydrotestosterone (DHT) produced in the gland by the reduction of testosterone through the action of specific enzyme, 5α reductase (Luke and Coffey, 1994; Thompson, 2001). The action of this androgen is mediated through specific binding of DHT to androgen receptors located on the epithelial cells of the gland (Chaves et al., 2012). However, abundant evidence now proves that estrogen, mediated through its two receptors, estrogen receptor alpha (ERα) and beta (ERβ) may also play a role in the development and perhaps, the functioning of the vesicular gland (Pelletier et al., 2000; Williams et al., 2001; Walker et al., 2012). Recent reports indicate that these receptors do not only mediate endogenous estrogen, but also mediate the toxicological and pathological effects of exogenous estrogen as well as interference with androgen action as a result of early-life estrogenic exposure (Walker et al., 2012). According to Joseph et al. (2011), the cellular presence and location of these receptors in the vesicular gland differs from one species of animal to another. In the rat vesicular gland (Pelletier et al., 2000), whilst ERα was observed more in the epithelial nucleus and less in the epithelial cytoplasm and nucleus of the stromal cells, ERβ showed weak epithelial nuclear labeling. Although present in the vesicular gland of mice, significant increases in cytosolic ER levels have been reported following neonatal exposure to Diethylstilbestrol (DES) (Turner et al., 1989; Walker et al., 2012). Therefore, the knowledge of the presence, location and distribution of these receptors is basic to understanding how estrogen affects this gland particularly in wild rodents undergoing domestication.

The greater cane rat (Thryonomys swinderianus), popularly known as Grasscutter, is a wild hystricomorphic rodent that is vigorously hunted and exploited for food in most part of West Africa. It provides veritable alternative protein source for both urban and rural populace (Addo et al., 2007). Though currently undergoing domestication and captive rearing, the recent trend in its farming is towards increased stock levels and intensification of production practices (Adu et al., 2005).

Although the morphology of the vesicular gland has been studied in few wild rodents like the African giant rat (Oke and Aire, 1997), Chinchilla (Adaro et al., 2001), Anantolial souslik (Cakir and Karatas, 2004) and Viscacha (Chaves et al., 2012), there is little or no information on either the structure or characterization of estrogen receptors in the vesicular gland of the cane rat. The present work therefore describes the structural and ultrastructural features as well as immuno-localize the estrogen receptors (ERα and β) in the vesicular gland of the cane rat. These will aid further research, facilitate future physiological and pathological studies while providing basis for functional interpretation of this gland in the reproductive biology of the male greater cane rat.

MATERIALS AND METHODS

Animals

Captive-reared, sexually mature male greater cane rats (*n=15*), with known reproductive and medical records were used in this work. Ten of the animals (10) were used for morphological and morphometric studies while five (5) were for immunohistochemistry. All the animals were still being used for breeding and were fed commercial cane rat feed and elephant grass with water *ad libitum.* The experimental protocol and animal handling followed the ethical principles in animal research adopted by the Council on Animal Experimentation of the University of Ibadan, Nigeria.

Gross evaluation and measurements

Each animal was weighed, anaesthesized and opened up after transcardial perfusion-fixation using the Karnovsky's fluid (phosphate buffered 2% paraformaldehyde – 2.5% glutaraldehyde fixative at pH 7.4) for the 10 animals meant for morphological studies and phosphate buffered 4% paraformaldehyde at pH 7.4 for the 5 animals meant for immunohistochemistry. After opening the abdominal and pelvic cavities, the pelvic symphysis of each animal was disarticulated to view the position and relations of the vesicular gland. The gland was then separated and dissected away from the other accessory sex glands, weighed (with its secretory content), measured (for volume, length using a ruler) and photographed (Samsung Digital camera, S100, Japan) for gross tissue assessment.

Histology and histometry

The samples for histological study were further fixed in Karnovsky's fixative, dehydrated in graded series of ethanol, cleared in xylene and embedded in paraffin. 5μm thick sections were mounted on albuminized slides, stained with Haematoxylin & Eosin and studied under Axioskop 2 plus, Carl Zeiss light microscope (Germany). Histo-

morphometric measurements of secretory unit diameters and epithelial heights were also done on these slides using a photomicroscope (Axio-Skop-2-Plus, ZEISS, Germany) with AxioVision Release 4.8.1 software package. Values obtained were expressed in mean ± standard deviation (*n = 10*) and subjected to correlation analysis using Microsoft Excel® data analysis tool.

Electron microscopy

The samples were further immersed in Karnovsky's fixative, postfixed in 1% osmium tetraoxide for 1hour, dehydrated in an increasing ethanol series, infiltrated and embedded in Epon-Araldide resin. Semi-thin and ultrathin sections were cut with an Ultracut S ultramicrotome. While the semi-thin sections were stained with Toluidine blue-Pyronin Y mixture and examined under light microscope, the ultrathin sections were mounted on copper grids, double-stained with uranyl acetate and lead citrate and observed in a Phillips CM10 transmission electron microscope (TEM).

Immunohistochemistry for estrogen receptor alpha and estrogen receptor beta

Five μm thick vesicular gland tissue sections were first deparaffinized and rehydrated in decreasing ethanol concentrations. To retrieve the Estrogen (α and β) antigens, the sections were heated in citrate buffer-Tween 20 solution in the microwave oven (DMO 289, Defy, South Africa) set at 720W for 10minutes and thereafter washed thrice in Tris buffered solution (TBS). The endogenous peroxidase was inhibited by treating the sections for 30minutes with 3% hydrogen peroxide (H_2O_2) obtained from the Novocastra™ kit (Peroxidase Detection System; RE 7110-K, Novocastra, UK) and thereafter washed thrice in TBS.

Nonspecific binding sites for immunoglobulins were blocked by incubating sections for 20 minutes in pre-constituted protein blocking solution (RE 7102, Novocastra™ kit). Upon washing in TBS, the sections were then incubated overnight at 4°C with 1:100 dilution of 1µl rabbit polyclonal for Estrogen receptor alpha (ERα – Ab37438, Abcam®, UK) and Estrogen receptor beta (ERβ – Ab3577, Abcam®, UK) on separately labelled slides. Sections were rinsed in TBS and treated for 30 min at room temperature with 1:300 dilution of biotinylated goat-anti-rabbit secondary antibody (Vector, USA) made in TBS. Sections were subsequently incubated with Streptavidin-Horse Radish Peroxidase mixture (RE 7104 Novocastra™ kit), for 30minutes at room temperature. The mixture contained 1-1.4µg of Streptavidin-HRP in 1ml Tris-buffered saline with protein stabilizer and 0.35% Pro-Clin™ 950. Peroxidase was developed with 1.74% (w/v) 3'3- diaminobenzidine (DAB) and 0.05% (v/v) H_2O_2 in Tris buffered saline (TBS). Finally, the immunostained sections were counterstained with Haematoxylin. Negative controls were obtained by incubating additional sections with the TBS in place of the primary antibody.

RESULTS

Macroanatomy and histology of the vesicular gland

The vesicular gland in the greater cane rat is a paired transparent and elongated tube, 5.3 ±1.16cm long, 1.03 ±0.5 cm³ in volume and weighing 1.15 ±0.67g which constituting 0.05% of the body weight (Table 1). It is located dorsal to the urinary bladder and anterior to the prostate and coagulating glands on either side of the midline (Fig. 1A). Each gland, which anteriorly deviates from the midline, has short finger-like branches but posteriorly converges with the other gland at about the midline to give a Y-shaped outline (Fig. 1B).The branches on each anterior part was 0.5cm in length with pointed extremities, while the unbranched posterior part of the glands tapers into duct that open separately into the
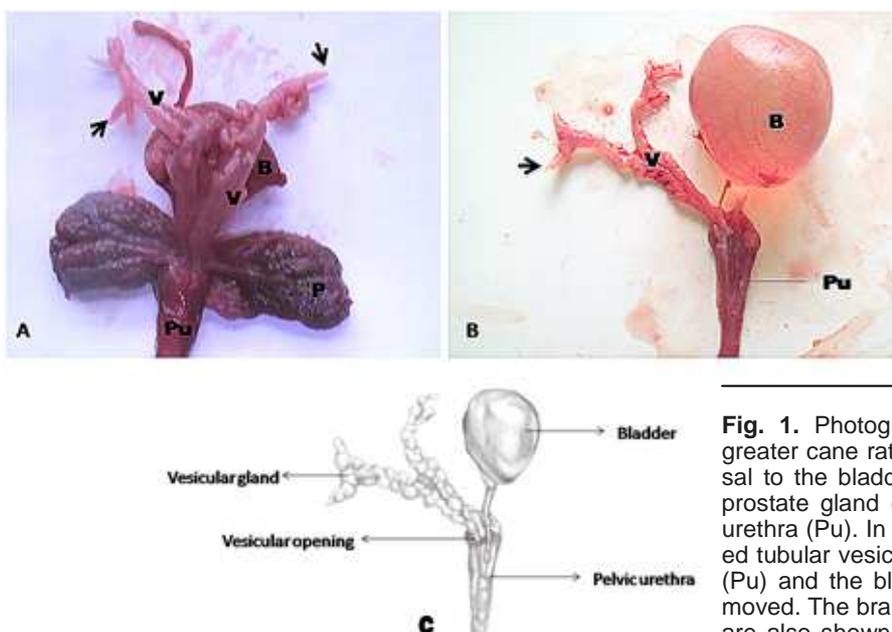

Fig. 1. Photographs of the vesicular gland in the greater cane rat. In **(A)** note the gland (V) lying dorsal to the bladder (B) and anterior to the reflected prostate gland (P) as they all open into the pelvic urethra (Pu). In **(B)** note the opening of the elongated tubular vesicular gland (V) into the pelvic urethra (Pu) and the bladder (B) with the other glands removed. The branches of the cranial part of the gland are also shown (arrows). **(C)** is the schematic diagram of the vesicular gland.

pelvic urethra (Fig. 1B). The colorless secretions contained within the gland become viscous to gel-like or even solid when exposed.

Histologically, the tubular glandular tissues of the vesicular gland in the cane rat are composed of three radially arranged layers: mucosa, muscularis, and adventitia (Fig. 2A). The mucosa was thrown into branching and anastomosing folds resulting in the formation of cavities and recesses with the mucosa (Figs. 2A, C). The fold, with a mean height of 321.53 ±70.26 μm, consists of a secretory epithelium and a thin underlying lamina propria, appeared more abundant in the anterior branched part almost completely occluding the lumen, than the posterior (Fig. 2C). The simple cuboidal epithelium is about 12.64 ±1.90 μm high and contains predominantly principal cells with scarce basal cells (Figs. 2B, D). These principal cells had their nuclei located at the base perpendicular to the lamina propriae, with moderately condensed chromatin and a conspicuous nucleolus (Figs. 2B, D). Each nucleus measures 5.43 ±0.57 μm in diameter (Table 1). Under the light microscope, all these cells appear almost similar, including the Toluidine (Figs. 2C, D). The few basal cells that rest on the epithelial basal lamina had eccentric nuclei with no nucleolus (Figs. 2D, 3). The lamina propria composes mainly of loose connective tissue with fibroblasts, collagen and elastic fibers. The muscular layers which is averagely 287.40 ±62.38 μm thick are made up of circular and longitudinally arranged smooth muscle fibres,

Table 1. The gross and histometric values of the Vesicular gland in the greater cane rat

	Mean ± Standard Deviation
Body weight (kg)	2.23 ±0.40
Vesicular weight (g)	1.15 ±0.67
Vesicular volume (cm^3)	1.03 ±0.50
Vesicular length (cm)	5.30 ±1.16
Vesicular epithelial height (μm)	12.64 ±1.94
Vesicular luminal diameter (μm)	919.47 ±125.13
Vesicular nuclear diameter (μm)	5.43 ±0.57
Vesicular muscular diameter (μm)	287.40 ±62.32
Vesicular fold height(μm)	321 ±70.26

collagen and elastic fibres as well as blood vessels surrounded by connective tissue adventitia (Figs. 2A, C).

Ultrastructure of the vesicular gland

Two variants of principal cells can be distinguished according to their electron density and cytoplasmic characteristics; the light principal cells (LPC) and the dense principal cells (DPC) (Fig. 3). Both cell types extend from the basement membrane to the glandular lumen and their luminal surfaces are studded with microvilli (Figs. 4A, B). At the lateral plasma membrane beneath the luminal surface, the cells are joined by tight junction followed by other junctional complex (Figs. 3, 4A). The light principal cells (LPC), which are more predominant, are columnar and relatively less dense containing coated vesicular granules and apical
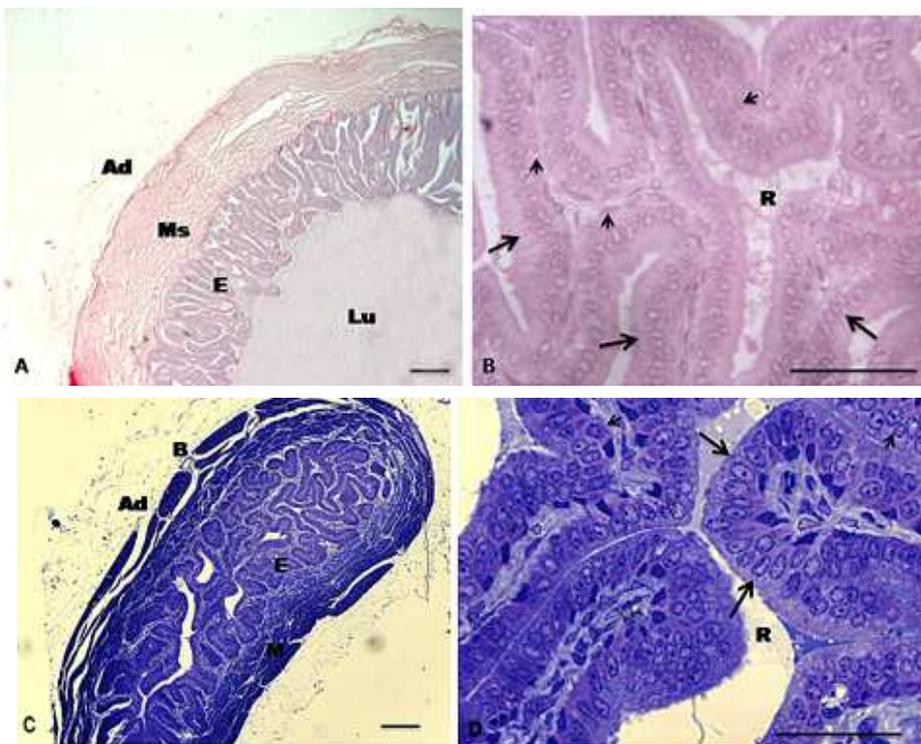

Fig. 2. Histology of the walls of the vesicular gland **(A)** and the glandular epithelium **(B)** of the greater cane rat. Note the adventitia (Ad) with some blood vessels, the muscle layers (Ms) and the folded epithelium (E) with the recesses as well as the glandular lumen (Lu). The glandular epithelium (Fig. B) with the principal cells (large arrows) and the scarce basal cells (small arrows) as well as the recess (R) formed by the mucosa folding. Fig. **(C)** is the cranial branch of the vesicular gland showing similar layers and the folded epithelium (E) that almost completely occluded the glandular lumen. Fig. **(D)** shows the glandular epithelium with the columnar princi-

pal cells (large arrows) and the scarce basal cells (small arrows) as well as the recess (R) formed by the mucosa folding. H & E staining (A,B), Toluidine Blue (C,D). Scale bars: A, C = 50 μm; B, D = 25 μm.
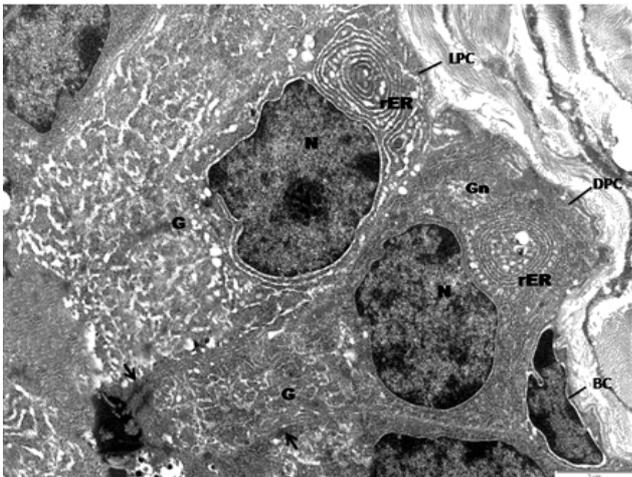
Fig. 3. The ultrastructure of the two principal cells in the vesicular gland of the greater cane rat. The light principal cell (LPC) and the dense principal cell (DPC) as well as the basal cell (BC) of the vesicular gland. Note the elaborate rough endoplasmic reticulum (rER), the Golgi complex (G), glycogen (Gn) the nucleus (N) and the junctional complexes (arrows) holding the cells. Scale bar: 2 µm.
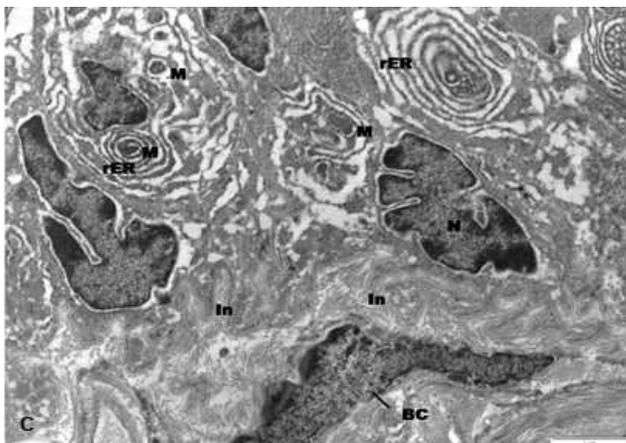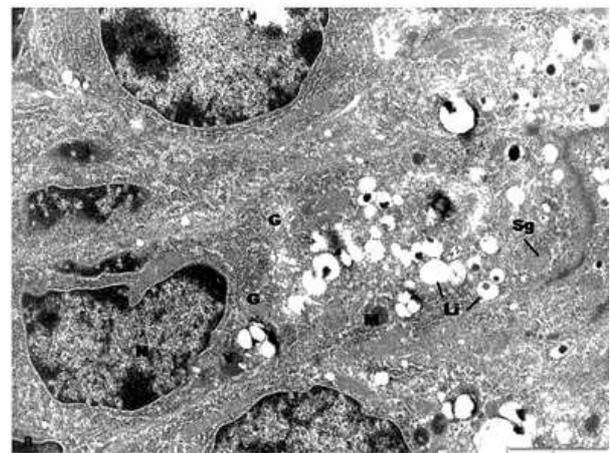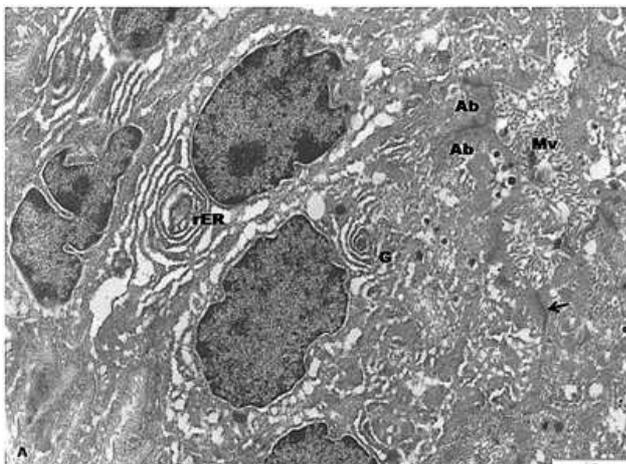

Fig. 4. Electron photomicrographs of the ultrastructure of light principal cells (LPC) of the vesicular gland in the greater cane rat. In (**A**) note the apical bleb (Ab) the abundant microvilli (Mv), the Golgi (G), rough endoplasmic reticulum (rER) and the zonular occludens (arrow). (**B)** shows the apical part of the LPC with the presence of golgi (G) around the nucleus (N), mitochondria (M) the secretory vesicle (Sg) and abundant lipid droplet (Li). Figure **C** and **D** show the basal part of light principal cells (LPC). In (**C**), note the abundant mitochondria (M) with some surrounded by rough endoplasmic reticulum cisternae (rER), the interdigitations (In) between the basal cells (BC) and LPC. In (**D**) are the cisternae of the rER with dilated edges and small vesicles (V), abundant mitochondria (M), the interdigitations (In) as well as the nucleus (N) with prominent nucleolus (Nu). Scale bar: A,B, 2 µm; C,D,1 µm.

blebs. While the apical cytoplasm contains a lot of lipid droplets and secretory vesicles, the apical to supranuclear cytoplasm contains well developed Golgi complexes appearing as stacks of parallel elongated cisternae with dilated edges (Figs. 4B, D). The round, in-folded nucleus of LPC contains large conspicuous nucleoli and fine euchromatin with some heterochromatic areas usually associated with the nuclear envelopes (Figs. 3, 4A, B). One prominent feature of these cells is the presence of abundant mitochondria with some surrounded by the well-developed cisternae of rough endoplasmic reticulum (rER). The rER cisternae have dilated edges and small vesicles seems to originate from them (Figs. 3, 4B). Interdigitations and hemidesmosomes connect the basal plasma membrane of the LPC to the basal cells and the underlying basal lamina as well as maintain close contact among the cells (Figs. 4C, D).

The dense principal cells (DPC) seem more pyramidal and electron-dense than the LPC. They have abundant well developed Golgi complexes located at the mid-apical cytoplasm with less secretory vesicles and lipid droplets at the apical cy-
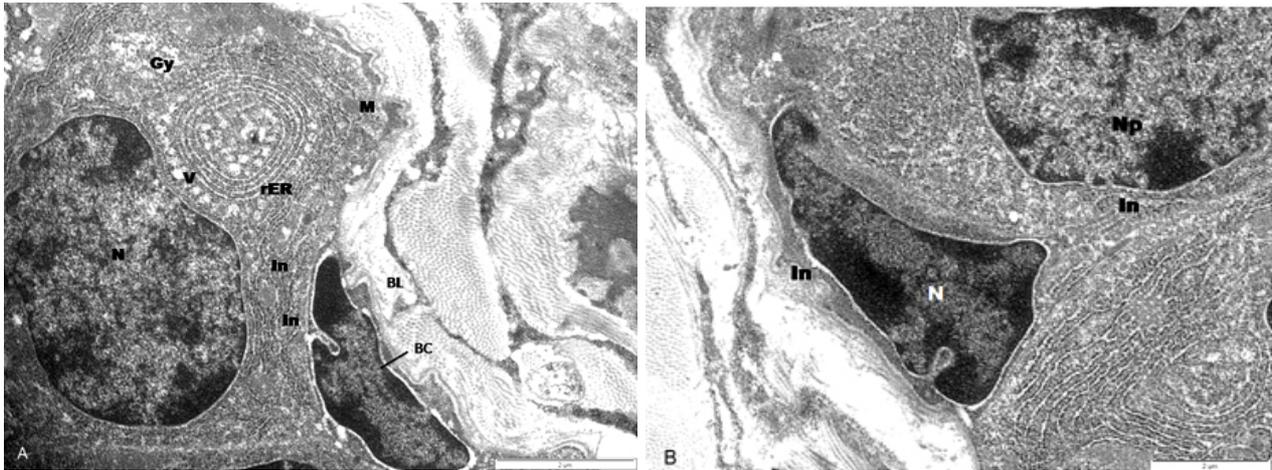
Fig. 5. Electron photomicrograph of the basal part of dense principal cell (DPC) and basal cell of the vesicular gland in the greater cane rat. Note in **(A)**, the mitochondria (M), the cisternae of rough endoplasmic reticulum (rER) with small vesicles (V), the interdigitations (In) between the DPC, basal cells (BC) and basal lamina (BL). Also note the fairly indented nucleus (N) and some glycogen residue (Gy). Indented nucleus (N) in Fig. **(B)** surrounded by scarce cytoplasm, the interdigitations (In) and the fairly indented principal cell nucleus (Np). Scale bar: A,B, 2 µm.
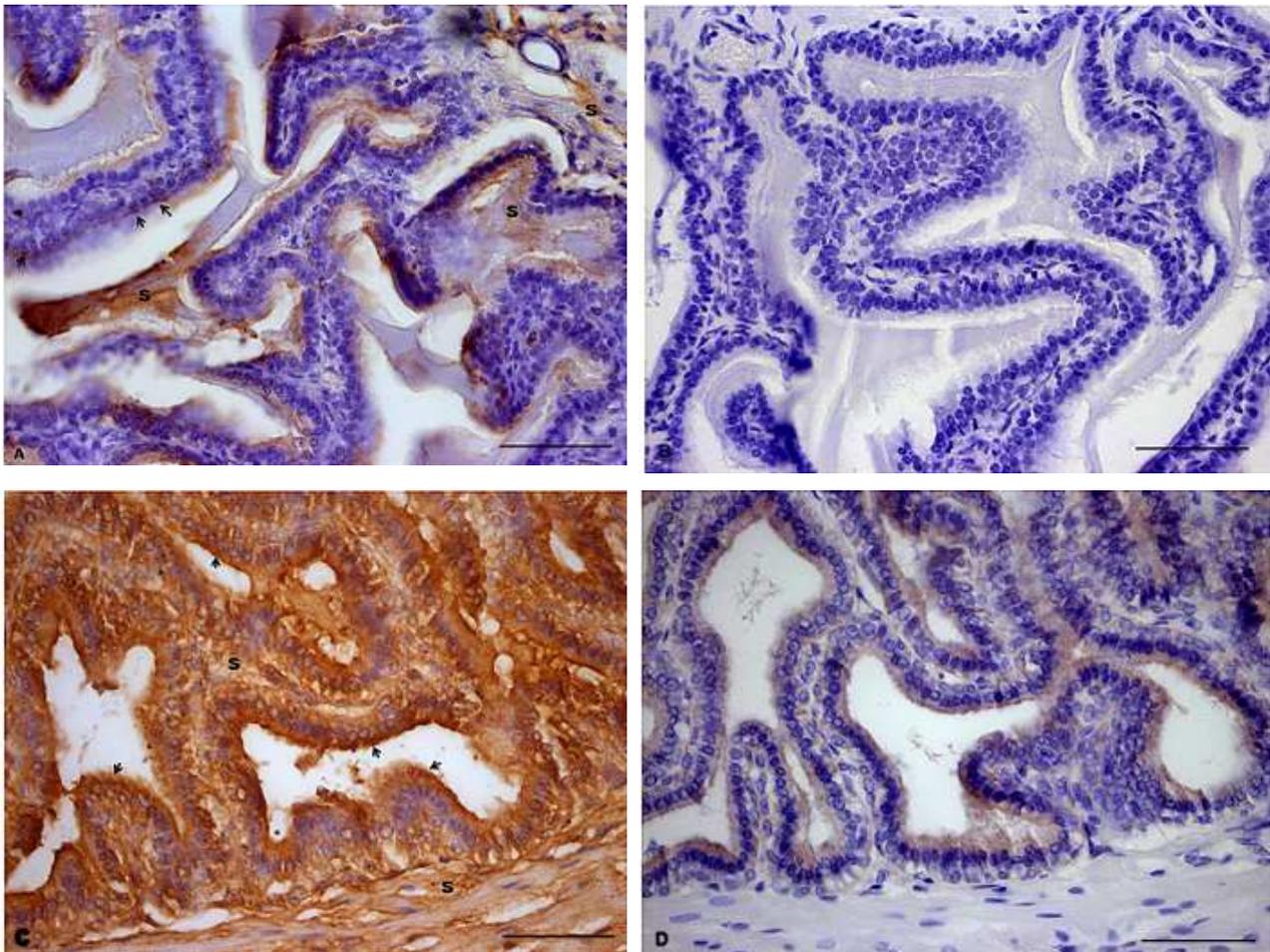

Fig. 6. Immunostaining for estrogen receptors in the vesicular gland in the greater cane rat. **(A)** Weak positive immunostaining of estrogen receptor alpha in the basal cell nuclei (arrows) and the stroma (S) and **(B)** is the negative control. **(C)** Strong positive immunostaining for estrogen beta receptor at both the cytosol and apical blebs (arrows) of the glandular epithelium as well as the stroma (S) and **(D)** is the negative control. Scale bar: A-D, 50 µm.

toplasm (Fig. 3). The rER is also well developed but restricted more to the basal cytoplasm and surrounded by secretory vesicles and mitochondria (Figs. 3, 5A). The fairly indented nucleus of the DPC is round and encloses granular dense euchromatin with heterochromatin areas that are either free or associated with the nuclear envelope. Just like the LPC, interdigitations and hemidesmosomes also connect its basal plasma membrane to the basal cells and the underlying basal lamina as well as maintain close contact with its LPC neighbor (Fig. 5A).

The basal cells are flat, wedged between the bases of two or more principal cells with flattened nuclei and scarce cytoplasm (Figs. 4C, 5). The invaginated nucleus encloses a granular uniformly distributed euchromatin with heterochromatic areas usually associated with the nuclear envelope with no prominent nucleolus (Fig. 5B).The cytoplasm has few cisternae of rough endoplasmic reticulum and mitochondria. Its apical and basal plasma membrane is related to the principal cells and basal lamina by interdigitations (Figs. 5A, B).

Estrogen receptor immunostaining in the vesicular gland

The vesicular gland in the cane rat showed positive immunostaining for both estrogen receptors alpha (ERα) & estrogen receptor beta (ER β). The ERα expression was located at the nucleus of the basal cells of the glandular epithelium and in the stroma (Figs. 6A, B) while the ERβ showed strong immunoexpression at the cytosol and apical blebs of the glandular epithelium as well as in the stroma (Figs. 6C, D).

DISCUSSION

The observed shape of the vesicular glands in the greater cane rat presents another variation in the morphology of this gland among the rodent species. Though branched tubular structure of the vesicular glands have been reported in two Neotropical hystricomorphic rodents, Agouti (Mollineau et al., 2009) and Paca (Ayres de Menezes et al., 2010), it is unique in the greater cane rat in that the branches are short and restricted to the cranial part of the gland.

The two types of columnar principal cells found in the secretory epithelium of the vesicular gland of the greater cane rat have been previously reported in the seminal vesicles of humans (Riva and Aumüller, 1994) and several mammalian species like Brazilian zebus (Cardoso et al., 1979), bulls (Amselgruber and Feder, 1986), buck and rams (Wrobel, 1970; Skinner et al., 1968), guinea pigs (Veneziale et al., 1974). According to Riva and Aumüller (1994), the difference in the histological appearances of the vesicular columnar cells could be attributable to the different stages of their secretory cycle. Therefore, while the light principal

cells of cane rat vesicular gland might represent the functionally differentiated cells, the dense principal cells may be referred to as 'aged' cells showing signs of cellular degeneration which is similar to the dense columnar cells found in seminal vesicle of pig (Badia et al., 2006).

The presence of well-developed rough endoplasmic reticulum and golgi apparatus, and the abundance of mitochondria seen in the principal cells of the vesicular glands in the greater cane rat, were similar to those reported in the seminal vesicle of rats (Murakami and Yokoyama, 1989), African giant rat (Oke and Aire, 1997), pig (Badia et al., 2006) and man (Riva and Aumüller, 1994). These suggest that principal cells of this gland are concerned with intense protein synthesis and secretions. As showed by Albert et al. (2002), large amount of ATP, at least four high-energy phosphate bonds are expended during protein synthesis. This enormous energy demand might explain the abundant presence of mitochondria in the cytoplasm of the principal cells. In addition, in the boar where eighty to ninety percent of the seminal plasma proteins are secreted by the seminal vesicles (Strzezek et al., 2000), some of the mitochondria are surrounded by the cisternae of the rough endoplasmic reticulum (Badia et al., 2006) similar to what we observed in the vesicular glands of the cane rat. Although the seminal plasma protein contribution from the vesicular glands in the greater cane rat is still being investigated, the vesicular glands might also be responsible for the bulk of the protein in the seminal plasma of the greater cane rat.

The observed microvilli, coated vesicles and interdigitation between the epithelial cells suggest the possibility of absorptive activities in the principal cells of the vesicular gland in the greater cane rat. In rats (Murakami and Yokoyama, 1989), pig (Badia et al., 2006) and man (Aumüller and Riva, 1992), the seminal vesicle has been reported to be involved with absorptive functions and in phagocytosis of spermatozoa. In pig seminal vesicle, the presence of microvilli and coated vesicles as well as presence of complex interdigitations between epithelial cells has been reported as evidences of their possible involvement in absorption and transcellular transport of materials stored in the gland lumen (Mata, 1995; Badia et al., 2006). The interdigitations observed between the epithelial cells and the stroma in the greater cane rat might suggest the existence of paracrine control between the stroma and the mucosa of the gland.

The structure and ultrastructure of the basal cell in the vesicular gland of the cane rat is consistent with that of most eutherine species. While the search for the exact function of the basal cells is still ongoing, different roles have been suggested for these cells. They could have structural role (Hayward et al., 1996), serve as reserve or stem cells of the columnar cells (Verhagen et al., 1988;

Riva and Aumüller, 1994) and could act as a potential mediator of luminal cell activity by regulating transport of material between secretory and stromal cells (El-Alfy et al., 2000). The presence of interdigitations between the principal cells, the basal cells and the stroma as well as the immunolocalization of the ERα in the basal cells suggests regulatory and structural roles for basal cells in the vesicular gland of the cane rat.

In the seminal vesicles of rat (Pelletier et al., 2000) and mice (Yamashita, 2004), immunostaining for ERα was reportedly found in the nuclei of epithelial and stromal cells. Similarly, in rat, weak staining for ERβ was localized in the epithelial cells of seminal vesicles even though ERβ mRNA could not be detected by in situ hybridization (Pelletier et al., 2000). In the same vein, significant increases in cytosolic ER levels have been reported in mice seminal vesicles following neonatal exposure to Diethylstilbestrol (Turner et al., 1989; Walker et al., 2012). Our findings revealed ERα immunostaining only of the basal cell nuclei and stroma in the cane rat vesicular glands. Also, the apical blebs of the glandular epithelium, the cytosol and the stroma all showed strong positive immunoreactivity to ERβ in the cane rat. According to Lazari et al. (2009), where there is close proximity of ERα positive stromal cells to epithelial cells as in the prostate, there is the possibility of paracrine effects of estrogens on the epithelium. It is therefore possible that estrogen may be involved in the normal functioning of the basal cells and stroma of the vesicular gland in the greater cane rat. However, further work is ongoing on the role of estrogen and its receptors in the normal functioning of the vesicular gland in the greater cane rat.

The viscous, gel-like nature of the vesicular glands secretion observed in the cane rat suggests they are involved in the formation of copulatory plug. Semen coagulation at the time of mating and copulatory plug formation observed in some rodents are products of complex biochemical interaction that involves the coagulation of a specific protein secreted by the seminal vesicles (Notides and Williams-Ashman, 1967; Parr et al., 1994). The nature and properties of the particular vesicular protein involved in this complex biochemical interaction in the cane rat awaits further study.

In conclusion, the present study highlights the structural and ultrastructural peculiarities, as well as the localization of the two estrogen receptors (ERα and β) in the vesicular glands of the greater cane rat. This information will provide basis for further morpho-functional analysis and detailed functional interpretations of this gland in the reproductive biology of the greater cane rat.

REFERENCES

Adaro L, Mendoza J, Cepeda R, Orostegui P (2001) Anatomo-radiographic study of the seminal vesicles of chinchilla (*Chinchilla laniger*) in captivity. *Rev Chil Anat*, 19: 297-300.

Addo PG, Awumbila B, Awotwi E, Ankrah NA (2007) Reproductive characteristics of the female grasscutter (*Thryonomys swinderianus*) and formulation of colony breeding strategies. *Livestock Res rural Develop*, 15: 1-3.

Adu EK, Otsyina RH, Agyei AD (2005) The efficacy of different dose levels of albendazole for reducing fecal worm egg count in naturally infected captive grasscutter (*Thryonomys swinderianus*, Temminck). *Livestock Res rural Develop*, 17: 1-6.

Alberts B, Bray D, Lewis J, Raff M, Roberts K, Watson JD (2002) Molecular Biology of the Cell. Garland Publishing, New York, pp 1463.

Amselgruber W, Feder FH (1986) Licht- und elektronenmikroskopische Untersuchungen der Samenblasendrüse (*Glandula vesicularis*) des Bullen. *Anat Histol Embryol*, 15: 361-379.

Aumüller G, Riva A (1992) Morphology and functions of the human seminal vesicle. *Andrologia*, 24: 183-196.

Ayres de Menezes DJ, Assis Neto AC, Oliveira MF, Miglino MA, Pereira GR, Ambrosio CE, Ferraz MS, Carvalho MA (2010) Morphology of the male agouti accessory genital glands (*Dasyprocta prymnolopha* Wagler, 1831). *Pesq Vet Bras*, 30: 793-797.

Badia E, Briz M, Pinart E, Garcia-Gil N, Bassols J, Pruneda A, Bussalleu E, Yeste M, Casas I, Bonet S (2006) Structural and ultrastructural features of boar seminal vesicles. *Tissue Cells*, 38: 79-91.

Cakir M, Karatas A (2004) Histo-anatomical studies on the accessory reproductive glands of the Anantolian Souslik (*Spermophilus xanthoprymmus*) (Mammalia: Sciuridae). *Anat Histol Embryol*, 33: 146-150.

Cardoso FM, Godinho HP, Nogueira JC (1979) Age-related changes in the seminal vesicles of a Brazilian (Nelore) zebu. *Acta Anat*, 103: 327-335.

Chaves EM, Aguilera-Merlo C, Filippa V, Mohamed F, Dominguez S, Scardapane L (2011) Anatomical, histological and immunohistochemical study of the reproductive system accessory glands in male viscacha (*Lagostomus maximus maximus*). Anat Histol Embryol, 40: 11-20.

Chaves EM, Aguilera-Merlo C, Crucen O, A., Fogal T, Piezzi R, Scardapane L, Dominguez S (2012) Seasonal morphological variations and age-related changes of the seminal vesicle of viscacha (*Lagostomus maximus maximus*): An ultrastructural and immunohistochemical study. *Anat Rec*, 295: 886-895.

El-Alfy M, Pelletier G, Hermo LS, Labrie F (2000) Unique features of the basal cells of human prostate epithelium. *Microsc Res Tech*, 51: 436-446.

Hayward SW, Brody JR, Cunha GR (1996) An edgewise look at basal epithelial cells: three-dimensional views of the rat prostate, mammary gland and salivary gland. *Differentiation*, 60: 219-227.

Joseph A, Shur BD, Hess RA (2011) Estrogen, efferent ductules, and the epididymis. *Biol Reprod*, 84: 207-217.

Lazari MFM, Lucas TFG, Yasuhara F, Gomes GRO, Siu ER, Royer C, Ferreira-Fernandes SA, Porto CS (2009) Estrogen receptors and function in the male reproductive system. *Arq Bras Endocrinol Metab*, 53: 923-933.

Luke M, Coffey D (1994) The male sex accessory tissue. Structure, androgen, action, and physiology. In: Knobil E, Neil J (eds). *The physiology of reproduction*. Raven Press, New York, pp 1435-1487.

Mata LR (1995) Dynamics of the seminal vesicle epithelium. *Int Rev Cytol*, 160: 267-302.

Mollineau WM, Adogwa AO, Garcia GW (2009) The gross and micro anatomy of the accessory sex glands of the male agouti (*Dasyprocta leporina*). *Anat Histol Embryol*, 38: 204-207.

Murakami M, Yokoyama R (1989) SEM observations of the male reproductive tract with special reference to epithelial phagocytosis. *Prog Clin Biol Res*, 296: 207-214.

Notides AC, Williams-Ashman HG (1967) The basic protein responsible for clotting of guinea-pig semen. *Proc Natl Acad Sci USA*, 58: 1991-2022.

Oke BO, Aire TA (1997) The epithelium of the vesicular gland of the African giant rat (*Cricetomys gambianus* Waterhouse): Histology and ultrastructure. *Afr J Med Sci*, 26: 69-72.

Parr MB, de Franca LR, Kepple L, Ying L, Parr EL, Russel LD (1994) The urethral glands of male mice in relation to depletion of secretory granules upon mating. *J Reprod Fertil*, 101: 675-680.

Pelletier G, Labrie C, Labrie F (2000) Localization of oestrogen receptor α, oestrogen receptor β and androgen receptors in the rat reproductive organs. *J Endocrinol,* 165: 359-370.

Riva A, Aumüller G (1994) Epithelium of the distal portion of the human spermatic pathway: seminal vesicle, ampulla ductus deferentis and ejaculatory duct. In: Motta P (ed.). *Ultrastructure of the Male Urogenital Glands: Prostate, Seminal Vesicles, Urethral, and Bulbourethral Glands*. Kluwer Academic Publishers, New York, pp 35-49.

Samuelson DA (2007) Textbook of Veterinary Histology. Saunders Elsevier, St. Louis Missouri, pp 418-441.

Skinner JD, Booth WD, Rowson LE, Karg H (1968) The post-natal development of the reproductive tract of the Suffolk ram, and changes in the gonadotrophin content of the pituitary. *J Reprod Fertil*, 16: 463-477.

Strzezek J, Martín-Rillo S, Saiz-Cidoncha F (2000) Glándula vesicular seminal del verraco: su papel en la capacidad de fertilización. *Anaporc*, 205: 59-84.

Thompson A (2001) Role of androgen and fibroblast growth factors in prostatic development. *Reproduction*, 121: 187-195.

Turner T, Edery M, Mills KT, Bern HA (1989) Influence of neonatal diethylstilbestrol treatment on androgen and estrogen receptor levels in the mouse anterior prostate, ventral prostate and seminal vesicle. *J Steroid Biochem*, 32: 559-564.

Veneziale CM, Brown ALJ, Prendergast FG (1974) Histology and fine structure of guinea pig seminal vesicle. *Mayo Clin Proc*, 49: 309-313.

Verhagen AP, Aalders TW, Ramaekers FC, Debruyne FM, Schalken JA (1988) Differential expression of keratins in the basal and luminal compartments of rat prostatic epithelium during degeneration and regeneration. *Prostate*, 13: 25-38.

Walker VR, Jefferson WN, Couse JF, Korach KS (2012) Estrogen receptor-α mediates diethylstilbestrol-induced feminization of the seminal vesicle in male mice. *Environ Health Perspect*, 120: 560-565.

Williams K, Fisher JS, Turner KJ, McKinnell C, Saunders PT, Sharpe RM (2001) Relationship between expression of sex steroid receptors and structure of the seminal vesicles after neonatal treatment of rats with potent or weak estrogens. *Environ Health Perspect*, 109:1227-1235.

Wrobel KH (1970) Zur Morphologie des Samenblasenepithels der Ziege. *Zentralbl Veterinarmed A*, 17: 634-643.

Yamashita S (2004) Ontogenic expression of estrogen receptor coactivators in the reproductive tract of female mice neonatally exposed to diethylstilbestrol. *Reprod Toxicol*, 18: 275-284.